



NON-INVASIVE CHARACTERIZATION OF MICROCRACKING, DAMAGE ACCUMULATION, AND PROPERTY DEGRADATION IN CORTICAL BONE USING LOW FIELD NMR

Daniel P. Nicolella¹, Qingwen Ni², and Kwai S. Chan¹

¹Mechanical and Materials Engineering Division and ²Space Science and Engineering Division
Southwest Research Institute®, San Antonio, TX

Introduction

Humans experience an age-related increase in the incidence of skeletal fractures and this increase may be due to a variety of factors including a decrease in bone mineral density, impaired balance and reflexes, changes in the shape and size of bones, changes in bone porosity and microarchitecture, alterations in bone mineral and organic constituents, and microdamage accumulation. The latter three factors, often referred to as "bone quality," are increasingly recognized as important determinants of fracture risk, especially for osteoporotic patients. Quantification of measures of bone quality such as microdamage accumulation, porosity, and pore size distribution may lead to a more accurate measure of bone strength and therefore fracture risk. Unfortunately, current technology does not allow the non-destructive and non-invasive detection of cortical bone microdamage or other measures of bone quality including microporosity. On the other hand, NMR proton spin-spin (T_2) or spin-lattice (T_1) relaxation time measurements and analytical processing techniques have been used to determine microstructural characteristics including porosity, pore size distribution, and permeability of various types of fluid filled porous materials with characteristic pore sizes ranging from sub-micron to sub-millimeter.

The objective of this investigation was to investigate changes in the low field pulsed NMR T_2 relaxation time distribution due to mechanically induce microdamage in cortical bone, and to use this information to predict the amount of damage and resulting material property degradation.

Methods

Overview of Experimental Methods:

1. Beam machined from human femurs 3mm x 5mm x 35 mm
2. Pre-damage NMR measurement
3. Cyclic four point bending fatigue loading to 20% or 30% stiffness reduction
4. Post-damage NMR measurement

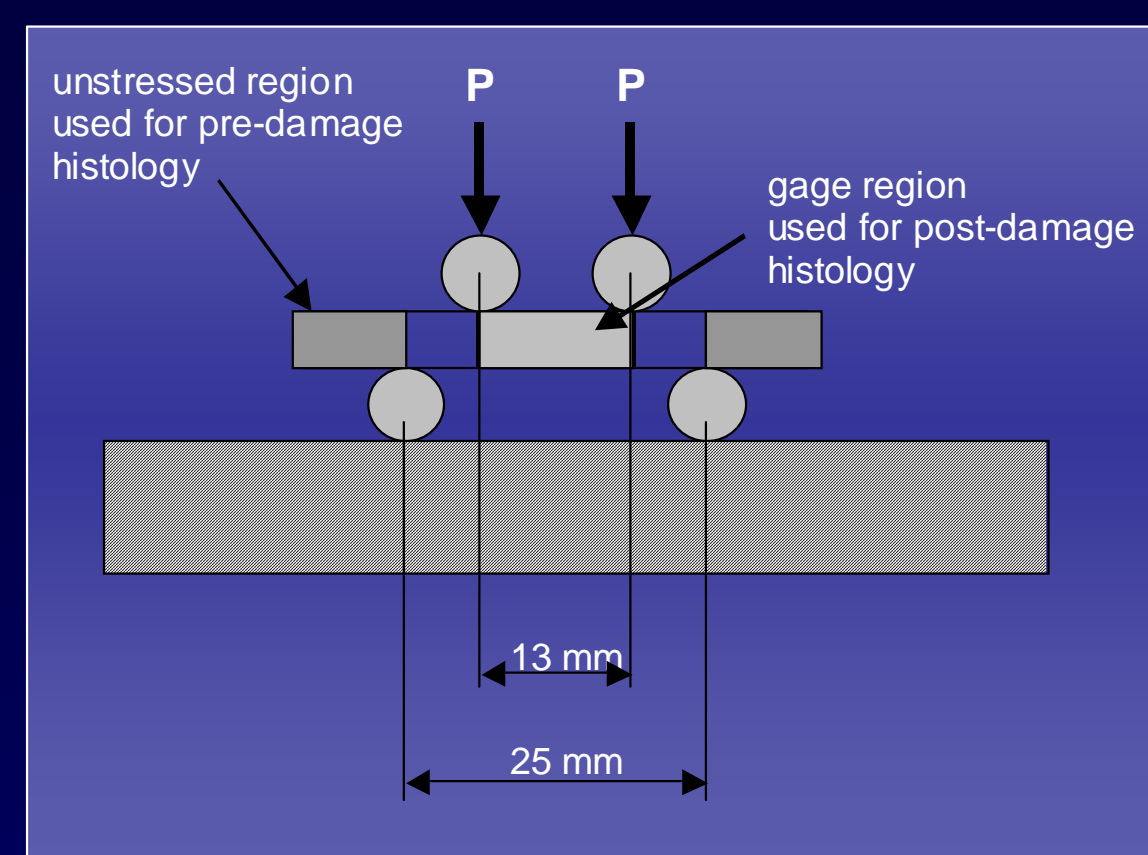


Figure 1. Four-point bending fatigue fixture. The portion of the specimen outside the lower loading pins remains unstressed during cyclic loading and was used for the pre-damage histology.

Four Point Bending

- Each specimen subjected to cyclic four-point bending (left) under load control
- The initial load was determined to produce 5000 microstrain in the outer fiber cyclically loaded until a 20% or 30% reduction secant stiffness
- All specimens were tested at 37°C in an environmentally controlled chamber under constant irrigation

NMR Measurement

- ^1H spin-spin profiles obtained by NMR CPMG [1, 2]:
 - $\{90^\circ - t - 180^\circ - (\text{echo})_n - T_R\}$ spin echo method
 - 9.0 μs for 90° pulse, t of 1000 μs , and T_R (sequence repetition rate) of 10s
- Inversion relaxation spectra related to pore size by [3, 4]:

$$\frac{1}{T_2} = \rho \left(\frac{S}{V} \right)_{\text{pore}}$$

- Inversion T_2 spectra peaks determined using non-linear least squares fit:

$$M = \sum_{i=1}^n \frac{1}{\sqrt{2\pi\sigma_i T_2}} \exp \left[-\frac{1}{2\sigma_i^2} (\ln(T_2) - \mu_i)^2 \right] w_i$$

Histomorphometric Analysis [5]

- Specimens bulk stained in basic fuchsin
- Mounted in plastic, cut, ground and polished to 80 μm thickness
- Imaged at 50X and 200X
- Haversian canal porosity determined from 50X image
- Lacuna porosity determined from 200X image
- Microdamage approximated as elliptical crack
- Porosity calculated as the total area of the pores (lacuna, Haversian canals and microcracks) divided by the total area of the image

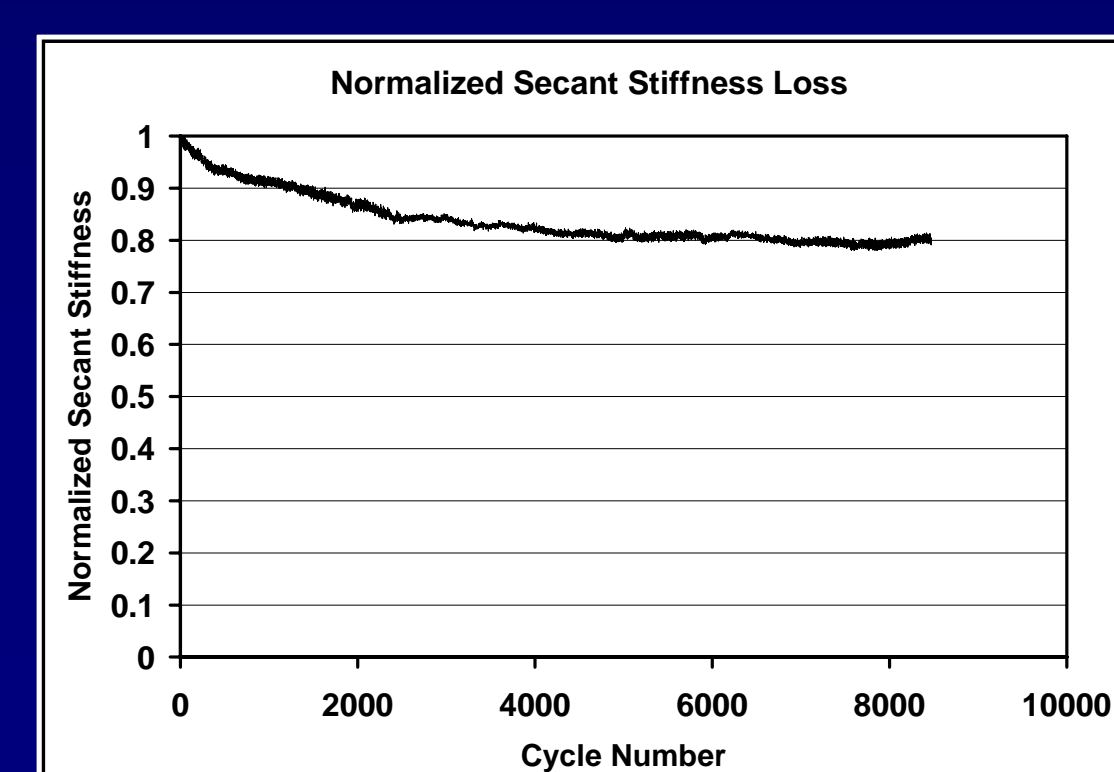


Figure 2. Typical normalized secant stiffness loss as a function of cyclic load number. The fatigue test was stopped when the specimen reached a 20% drop in stiffness.

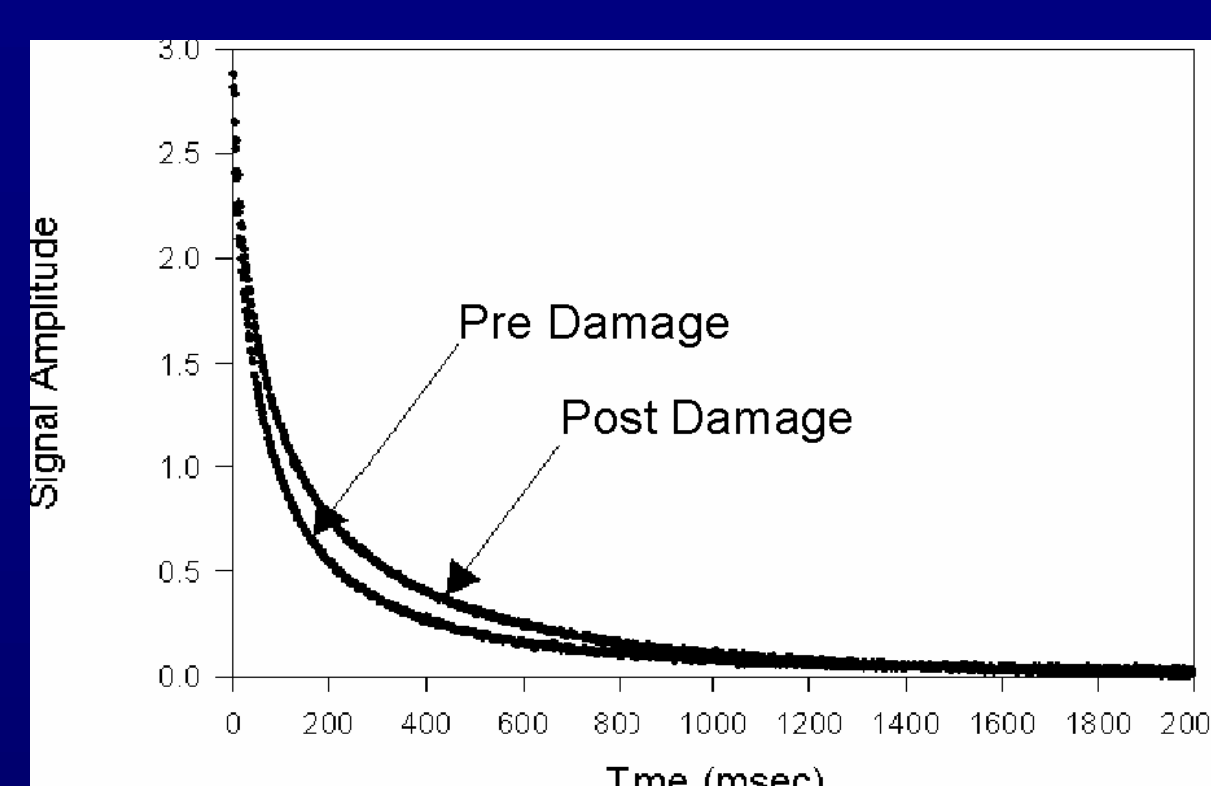


Figure 3. Pre- and post-damage NMR CPMG spin relaxation decay signals.

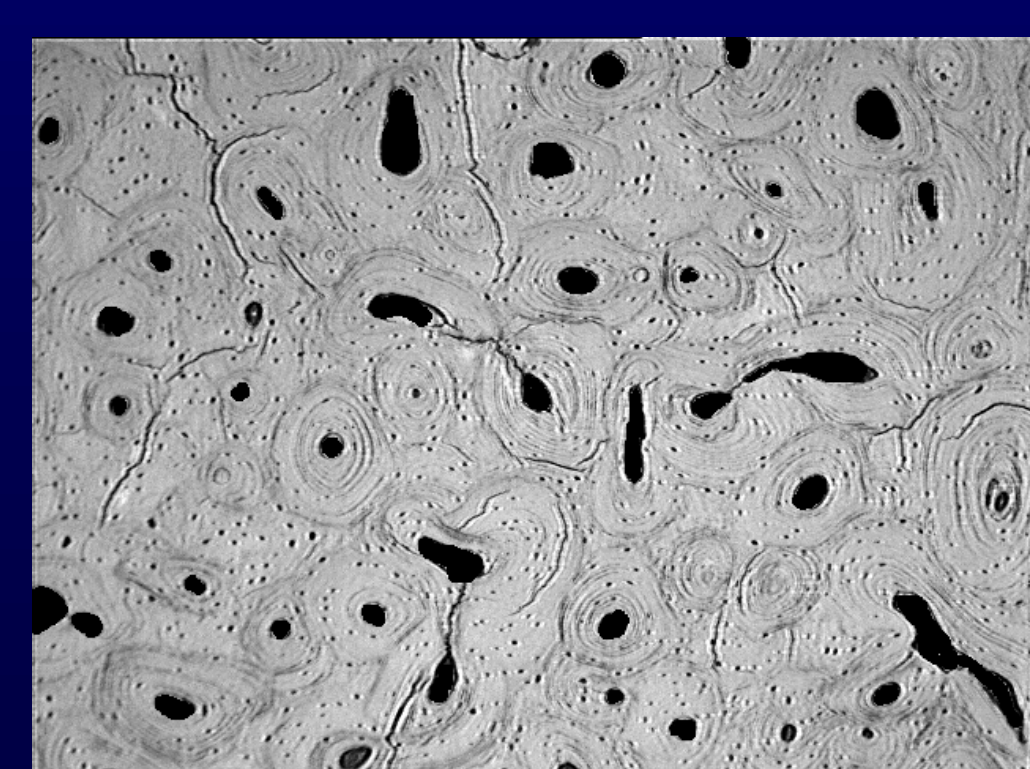


Figure 4. Post-damage optical micrograph (50X).

Methods (continued)

Crack Density (C_D) Determination from NMR Spectra

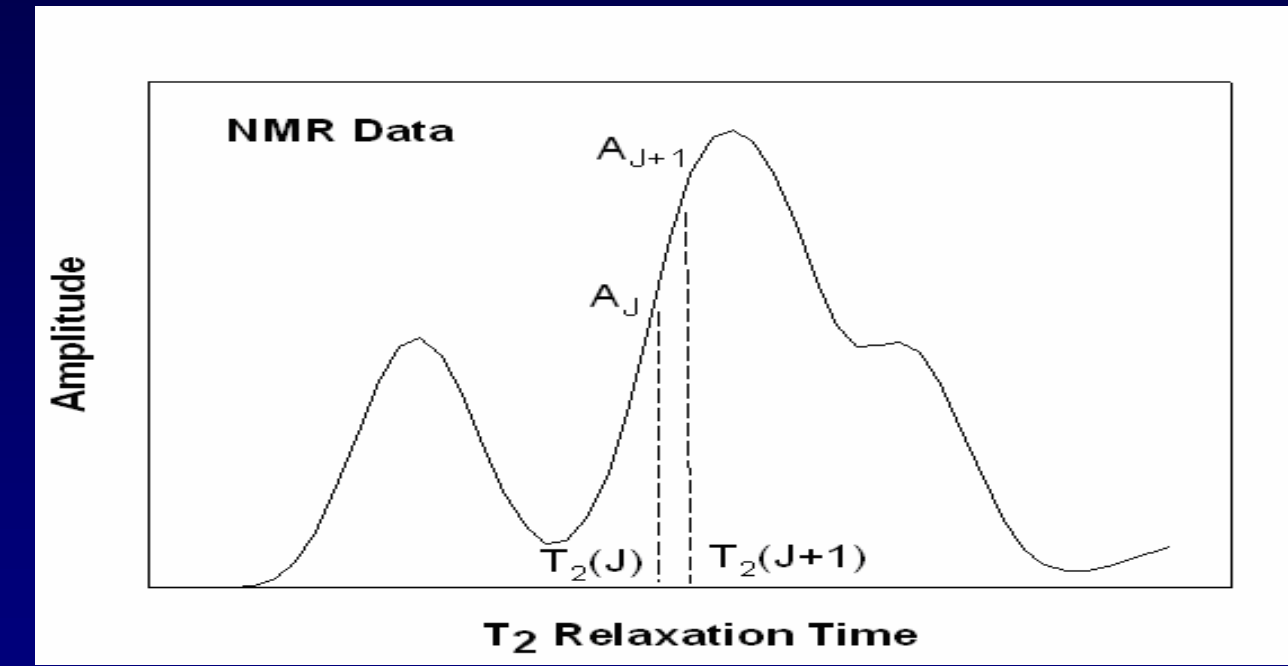


Figure 5. Determination of crack density from NMR spectra

- For an arbitrary $T_2(j)$, the pore radius, $r(j)$, is computed according to

$$r(j) = \rho Q T_2(j)$$

where ρ ($\rho = 0.25$) and Q ($Q = 6.41$ or 4) are pore size constants previously determined from NMR measurements [4, 5]

- The relative contribution of pores with radius $r(j)$ to the total pore volume

$$V_{\text{pore}}^i(j) = \frac{[A_{j+1}^i + A_j^i] V_{\text{total}}^i}{2[T_2(j+1) - T_2(j)] A_{\text{total}}^i}$$

where $V_{\text{pore}}(j)$ is the pore volume corresponding to $T_2(j)$. V_{total} is the total pore volume and A_{total} is the total area under the NMR- T_2 curve. The superscript i indicates quantities prior to damage when $i = 0$, and quantities after damage when $i = 1$

- The change in pore volume resulting from damage is then given by

$$\Delta V_{\text{pore}}(j) = V_{\text{pore}}^1(j) - V_{\text{pore}}^0(j)$$

which is considered to be the volume of microcracks, V_{mc} , created due to damage

- The volume of the microcracks is given by

$$V_{\text{mc}} = \frac{n}{V} \pi \delta a^2$$

where n is the number of microcracks; V is the total volume of the specimen; δ and a are the average crack opening displacement and the average crack radius

- The crack density parameter, C_D , is defined as

$$C_D = \frac{n}{V} a^3 \quad \text{leading to} \quad C_D(j) = \frac{a(j)}{\pi \delta(j)} \Delta V_{\text{pore}}(j)$$

where $\Delta V_{\text{pore}}(j)$ is obtained from NMR measurements

- For a semi-circular surface crack under elastic loading

$$\frac{\delta}{a} = 2\sqrt{3} \frac{(1-\nu^2)\sigma}{E} \quad \text{leading to} \quad C_D(j) = \left(\frac{2\sqrt{3}(1-\nu^2)\sigma}{\pi E} \right) \left[\frac{\sigma}{E} \right] \Delta V_{\text{pore}}(j)$$

- The degradation in elastic modulus due to damage accumulation is given by

$$\frac{1}{E^i} = \frac{1}{(1-D)^2} \left[\frac{1}{E^i} \right] \quad \text{where} \quad D = 1 - \left[1 + \frac{16(1-\nu^2)C_D}{3(1-\frac{4C_D}{9})} \right]^{-\frac{1}{2}}$$

Results

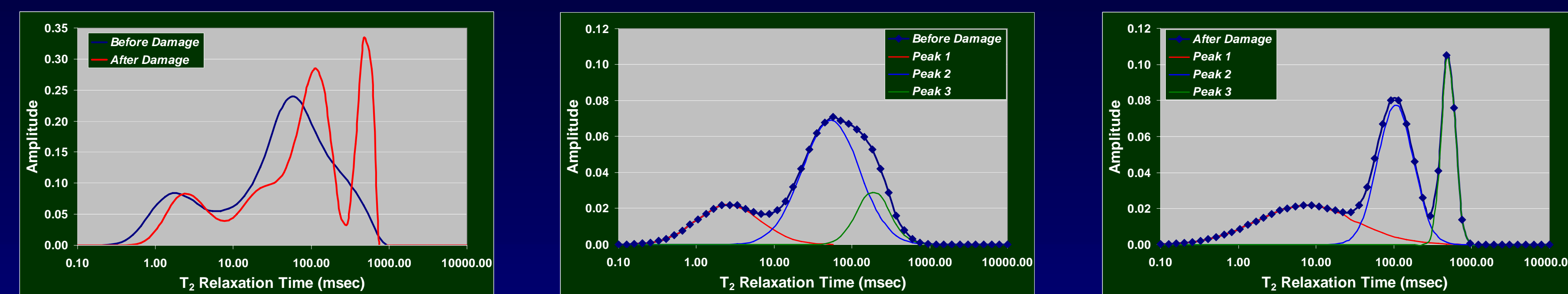


Figure 6. Left: Typical comparison of the inversion T_2 spectra between pre-damage and post-damage samples. Middle-left and middle-right: Individual inversion T_2 peaks representing smaller lacuna-sized, and larger Haversian and microdamage sized pores [4]. Tables at the right indicate changes in individual peaks due to microdamage. Using the surface relaxivity, the spatial domain of each peak can be quantified.

	Porosity	
	Pre-Damage	Post-Damage
total	10.50%	11.10%
peak 1	0.08%	0.43%
peak 2	7.25%	3.26%
peak 3	3.15%	7.39%

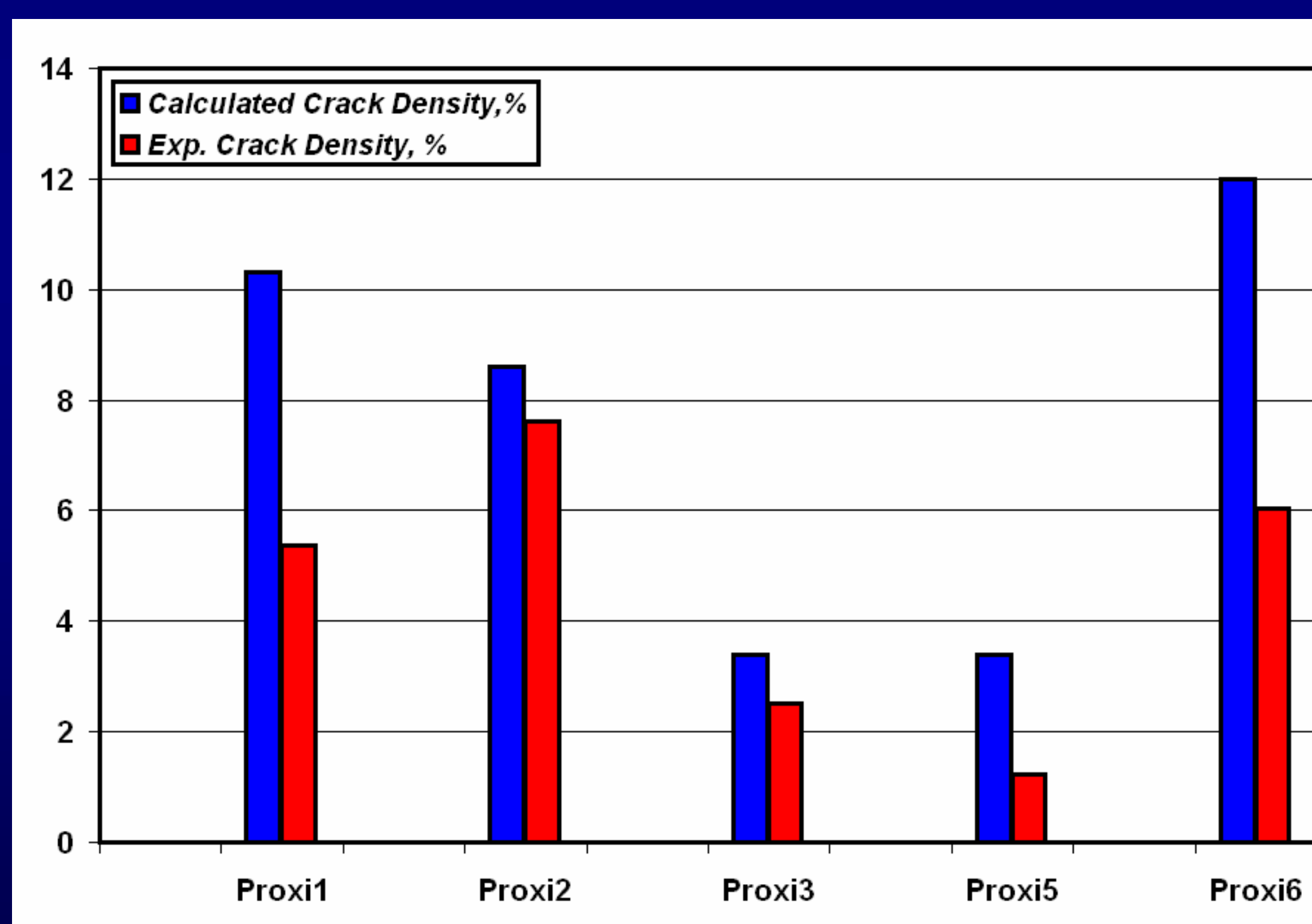
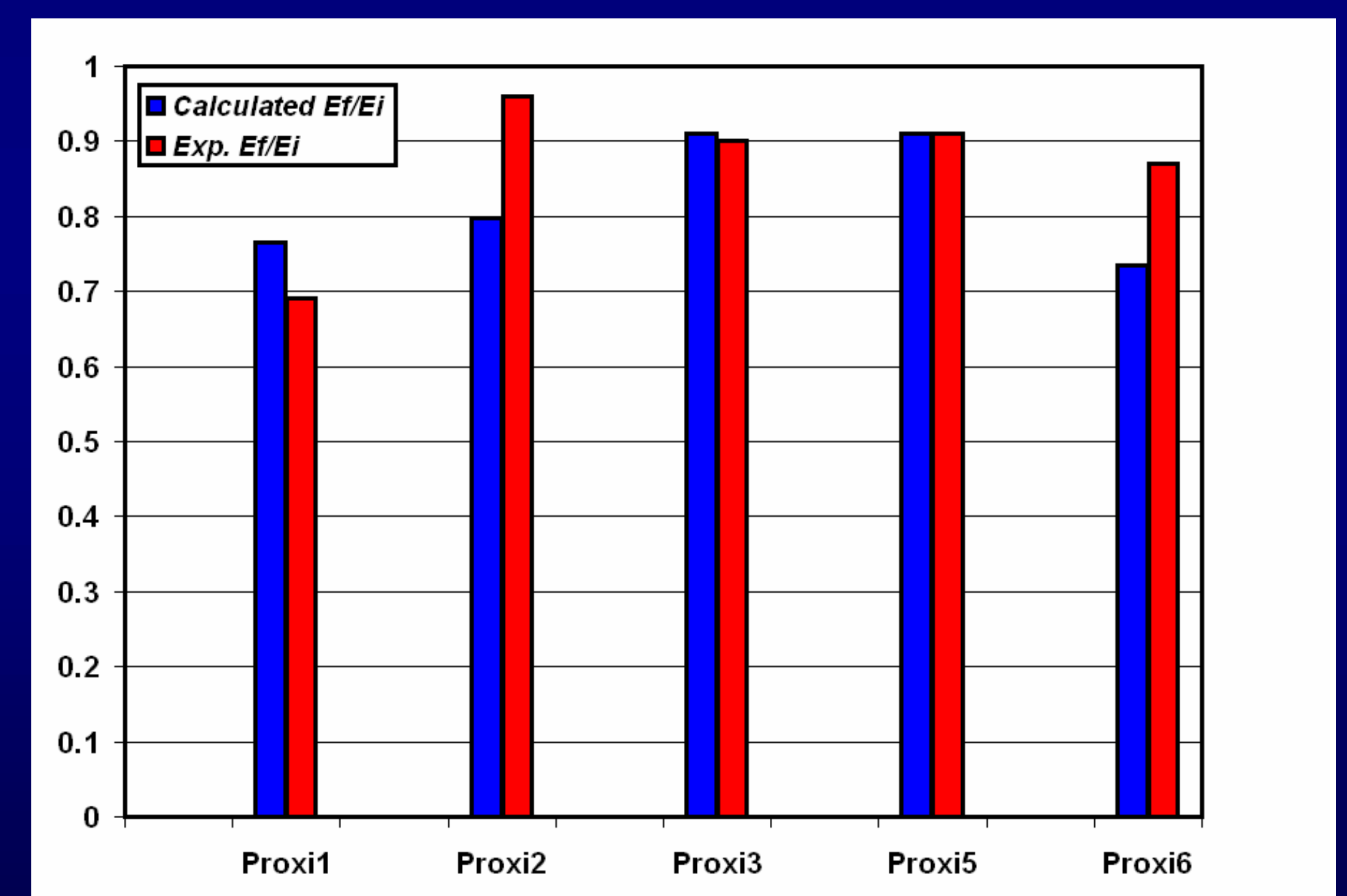


Figure 7. Left: Measured crack density determined from histomorphometry versus cracked density calculated from NMR spectra. Right: Experimentally measured modulus reduction versus modulus reduction computed from NMR spectra using NMR derived crack density. The histomorphometrically determined crack density is generally lower than the NMR derived crack density; the histology based method estimates crack density from a small number of thin slices while the NMR techniques measures the whole bone specimen.



Discussion

- NMR relaxation signal is altered due to the presence of microdamage in cortical bone when compared to undamaged bone
- Intrinsic porosity of the bone unchanged - alterations in the NMR T_2 relaxation signal due to induced microdamage
- NMR method is non-destructive, non-invasive, and provides 3D (bulk of sample) results
- Histomorphometry method is destructive; pore size is determined from cross sectional area, which varies with not only the size of the pores but also their orientations with respect to the cross section, crack distribution is non-homogeneous, and does not give actual 3D results
- By calibrating the surface relaxivity constant to a known porosity, the spatial domain of bone damage can be quantified
- Using this information and an assumed approximation of microcrack geometry, the effects of microdamage on mechanical property degradation can be calculated

Acknowledgements: This work was supported by NIH/NIAMS AR049627

References: 1). Carr, H.Y. and Purcell, E.M., Phys. Rev. 904, No. 3:630, 1954. 2). Meiboom, S., and Gill, D. Rev. Sci. Inst. 29, 1958. 3). Saadatmanesh, H., Ehsani, R. Insight Vol. 39, No. 2, 75, 1997. 4). Ni, Q. Derwin, K. and Wang X., 2004, Meas. Sci. Technol 15 58-66. 5). Ni, Q. and Nicolella, D.P., 2005, Meas. Sci. Technol 16 659-668.